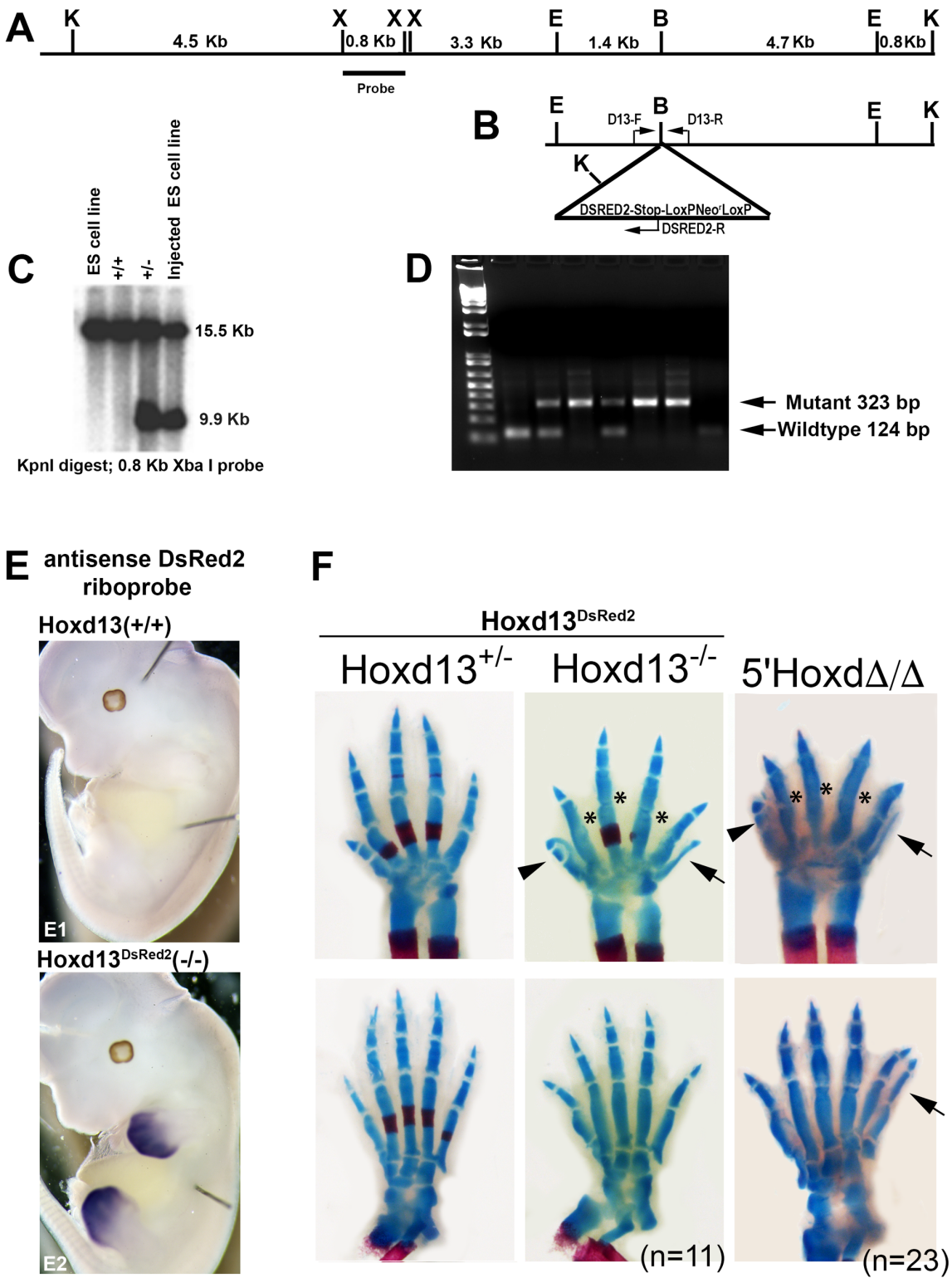

Figure S1. Production of the Hoxd13DsRed2 allele and characterization of mutant limb phenotypes. Related to Figure 1, and to STAR Methods.

(A) Restriction map of the *Hoxd13* genomic region. K= KpnI, X= XbaI, B= BamHI, E= EcoRI.

(B) Hoxd13DsRed2 gene targeting vector.

(C) Southern blot analysis of ES cell DNA following targeting vector electroporation and positive/negative selection. A 0.8Kb XbaI fragment was used as a probe to detect homologous recombination of the Hoxd13DsRed2 targeting vector which introduces a second KpnI restriction fragment length polymorphism at the targeted locus.

(D). PCR analysis of mouse tail DNA derived from heterozygous intercrosses of Hoxd13DsRed2 mice.

(E) *In situ* hybridization using a DsRed2 antisense riboprobe detects the expression of the DsRed2 transcripts in the *Hoxd13* expression domain in homozygous mutant embryos (E2) but not wild type littermates (E1), consistent with the placement of the Ds2Red Stop LoxP Neo LoxP cassette into exon 1 of *Hoxd13*.

(F) Skeletal staining of *Hoxd13* heterozygous and homozygous mutant Hoxd13Ds2Red littermate forelimbs (FL) and hindlimbs (HL) at E17.5 compared with 5'HoxdΔ/Δ homozygous mutants at the same stage. *Hoxd13*$^{-/-}$ limbs have loss of phalangeal joints (asterisks), malformation of FL distal digit 1 (arrowhead), and brachydactyly (digits 2 and 5) as previously reported for *Hoxd13* loss of function alleles. The 5'HoxdΔ/Δ has similar phenotypes, but with somewhat more severe forelimb brachydactyly and joint loss, and occasional digit duplication (arrows) in hindlimb, and postaxial forelimb condensation.

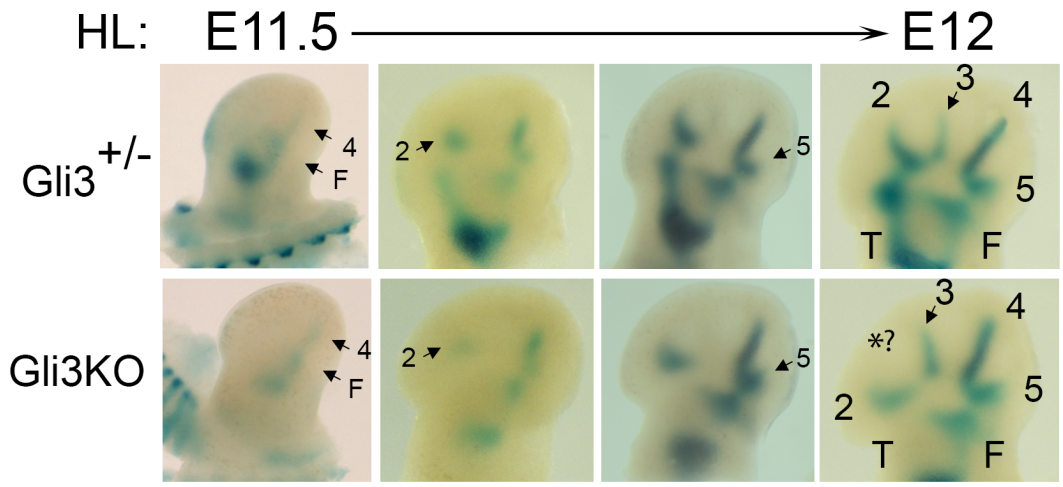

Figure S2. Primary limb axis forms with normal postaxial dominance in *Gli3* KO hindlimb buds. Related to Figure 2.

NogginLacZ staining of forming limb condensations in *Gli3*$^{-/-}$ (KO) hindlimb buds compared to *Gli3*$^{+/-}$ controls ranging from time E11.5-E12. Postaxial polarity in appearance order is preserved in zeugopod and digits, but with occasional late appearance of an additional anterior digit condensation between d2 and d3 (denoted by *). Note that preaxial expansion-digit duplication is less prominent in *Gli3* KO hindlimbs than forelimbs (shown in Figure 2).

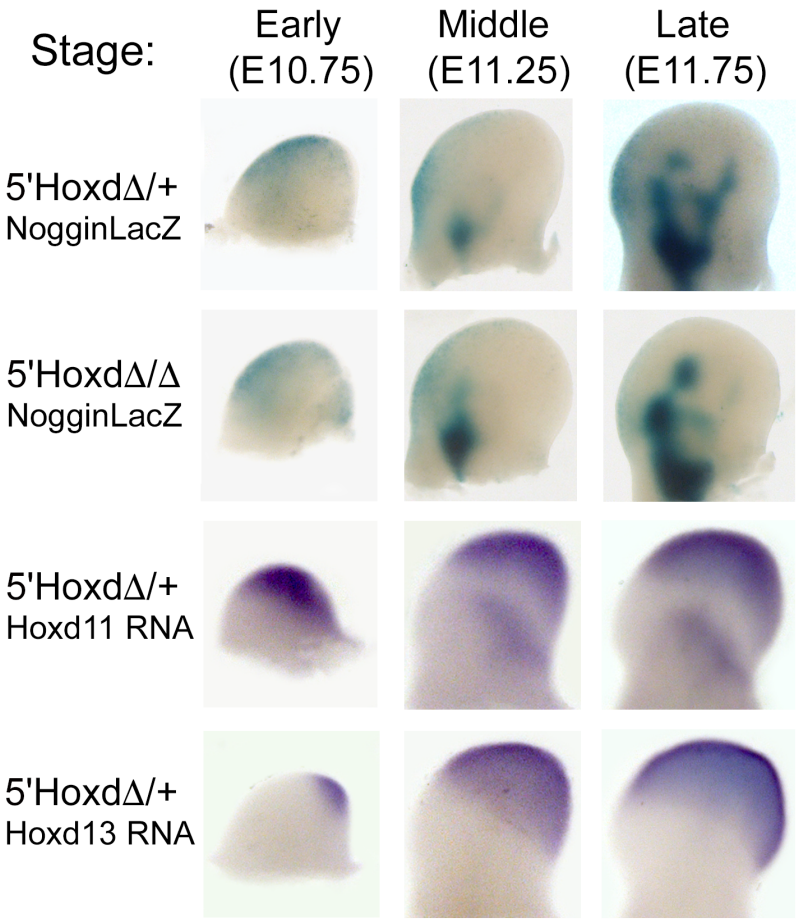

Figure S3. Condensations formed and Hoxd11, Hoxd13 expression domains at stages analyzed for condensation rates and for cell cycle parameters. Related to Figures 3, 4.

Hindlimb buds of control (wildtype or 5'HoxdΔ/+) and 5'*Hoxd* mutant (5'HoxdΔ/Δ) embryos were used for analysis of aggregation rates in high density cultures (HDC) and for cell cycle analysis of dissociated limb bud cells at the stages indicated, as described in text. At the early stage (E10.75), no condensations have formed and 5'*Hoxd* gene expression (*Hoxd11-Hoxd13*) is in phase one (posterior nested pattern). At mid-stage (E11.25, also used for HDC analyses), formation of the zeugopod condensation for the dominant primary limb axis is just initiating and 5'*Hoxd* expression is broadening across the anterior-posterior limb bud axis. At the late stage (E11.75), second phase 5'*Hoxd* expression is underway, with *Hoxd13* expression extending across the anterior-posterior limb bud. In all panels, limb buds are shown with anterior to left, posterior to right, and distal toward top.

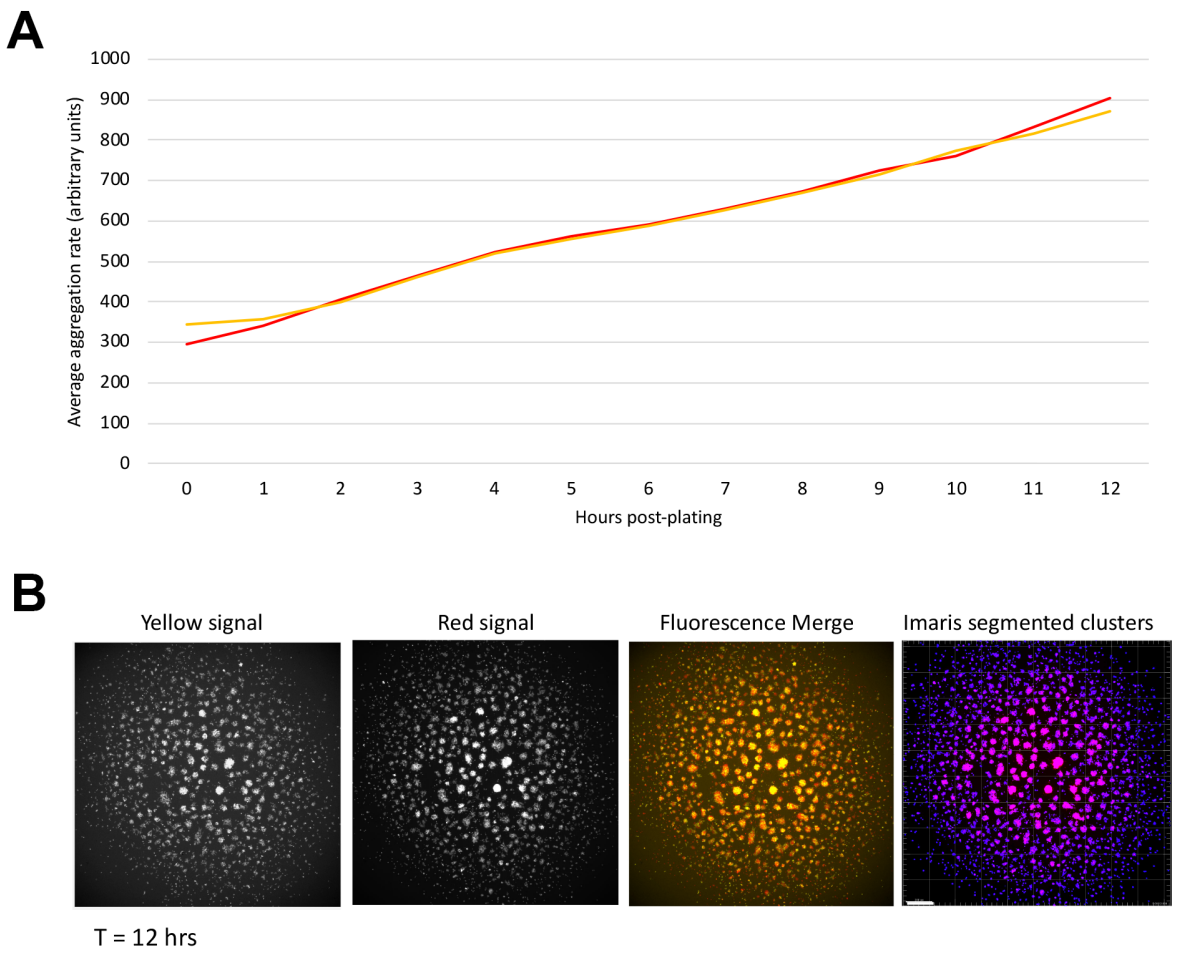

Figure S4. Example of Imaris calculations of average limb cell aggregate size at different times using Imaris software. Related to Figure 3.

The Imaris 'surfaces' tool was used to generate segregated clusters and calculate average aggregate sizes for still fluorescence images collected every hour during the first 12 hours of high density culture (HDC). The areas and numbers of segregated surfaces were determined at each time point.

(A) Example of data on aggregate sizes of clusters for yellow (EYFP) and red (TdTomato) fluorescence channels graphed over time (1-12 hrs).

(B) Example of segregated TdTomato clusters generated by Imaris for T=12 hrs (anterior WT-EYFP and WT-TdTomato cells in mixed HDC). Scale bar 200 μm.

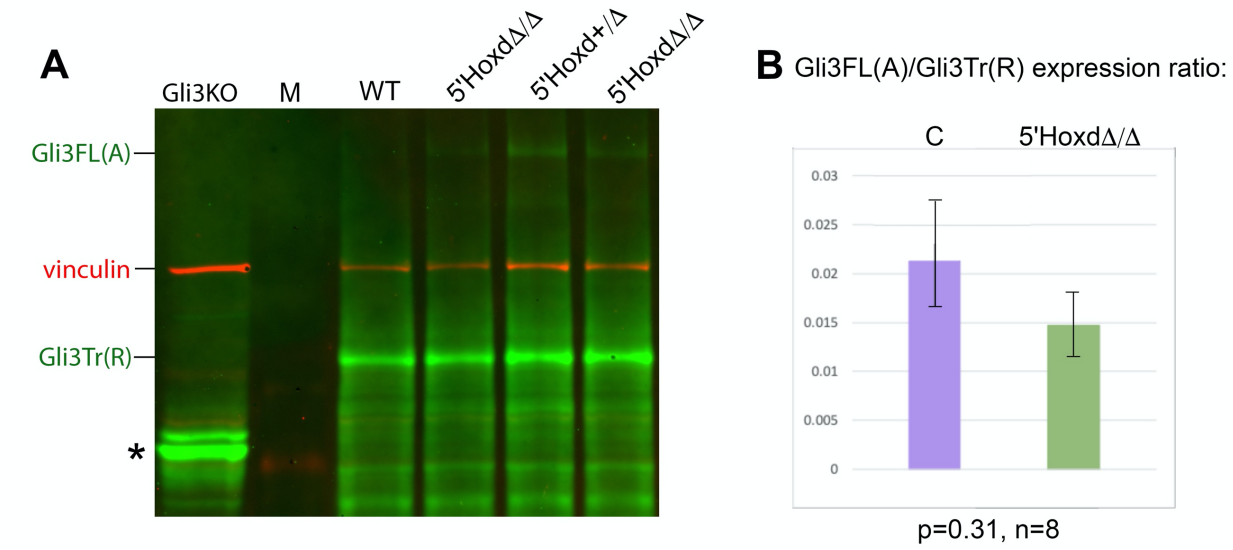

Figure S5. Analysis of Gli3 protein levels in control wildtype and 5'*Hoxd* mutant limb buds. Related to Figure 5.

Gli3 protein levels and Gli3 full-length (FL)/repressor (Tr) ratios (graph to right) are not significantly changed in 5'HoxdΔ/Δ compared to control (C) limb buds (hindlimb E10.75; N=8 each genotype) on immunoblots probed with anti-Gli3 (green) and with anti-vinculin (red) as a loading control for each lysate lane. *Gli3* KO (*Gli3*$^{-/-}$) limb bud was included as a negative control.

(A) Representative immunoblot showing E10.75 control (WT or 5'Hoxd+/Δ) and 5'*Hoxd* mutant lysates. In the middle two lanes, additional WT and mutant (5'HoxdΔ/Δ) samples are shown that were not included in the N=8 set analyzed, because these lanes were under-loaded and the Gli3FL band is faint and not easily measured accurately. Only lysates with clear Gli3FL and Gli3Tr bands were quantitated.

M, molecular weight marker lane. *, truncated Gli3 peptide with frame-shifted fusion protein produced by *Gli3* KO allele (*XtJ/XtJ* mutant).

(B) Graph showing the mean and SEM for the Gli3FL/Gli3R ratio. A total of 8 independent limb bud lysates each, for control (C) and for 5'HoxdΔ/Δ, were analyzed. Controls included seven WT and one 5'Hoxd+/Δ lysate. Difference was not significant using standard 2-tailed T test (p=0.31).

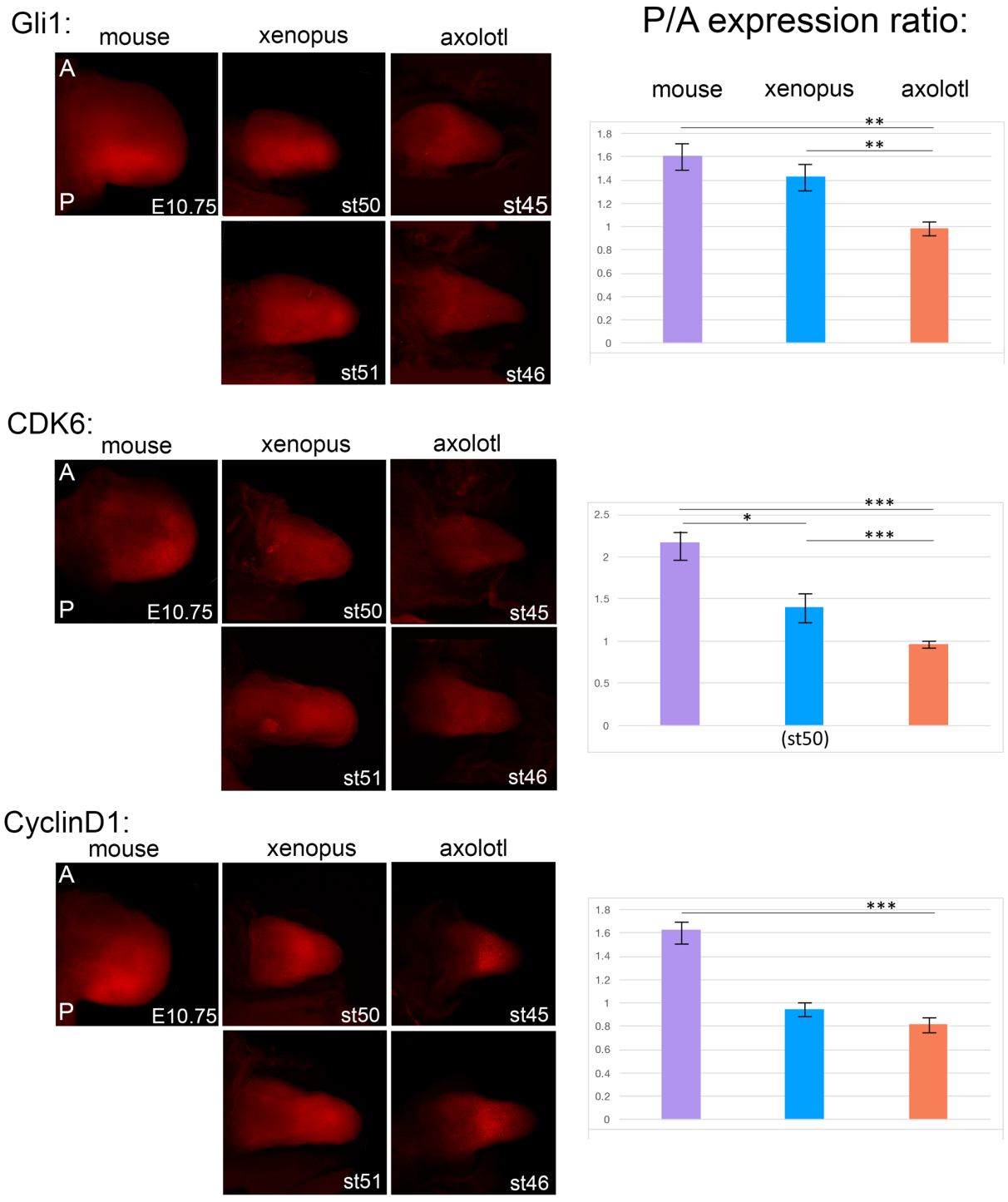

Figure S6. Relative posterior-to-anterior (P/A) levels of Gli3-regulated targets in xenopus and axolotl limb buds compared to mouse. Related to Figure 5.

Relative P/A expression levels of *Gli1*, *Cdk6*, And *CyclinD1* transcripts compared between wildtype mouse (E10.75 forelimb), *Xenopus* (stages 50-51 hindlimb) and axolotl (stages 45-46 forelimb) limb

buds detected using whole mount in situ hybridization chain reaction (HCR) and quantitated with confocal microscopy (as in Figure 5). All limb buds shown oriented with anterior (A) at top, posterior (P) at bottom, and distal to right side. Both mouse and *Xenopus* (stage 50 only for *Cdk6*), demonstrated polarized *Gli1* and *Cdk6* expression (P/A >1), consistent with graded Gli3R activity, whereas axolotl expression of all transcripts was uniform across the AP axis at both stages analyzed. *CyclinD1* expression was only highly polarized in mouse, but not in *Xenopus*. For each probe within a species, a minimum of 3 embryos were hybridized at the same time under uniform conditions and evaluated. Total fluorescence intensities in equally-sized and proximo-distally positioned anterior and posterior domains within a limb bud were measured using Image J software, and P/A ratios determined. Graphs to right show mean fluorescence P/A ratios and SEM. Significance determined using standard 2-tailed T test. *, $p<0.05$; **, $p<0.01$; ***, $p<0.001$.